X-ray optics of surfaces (reflection and diffraction at grazing angles of incidence)

A. V. Andreev

M. V. Lomonosov State University, Moscow

Usp. Fiz. Nauk **145**, 113–136 (January 1985)

A new direction in the field of x-ray optics is discussed. This new direction is associated with diffraction at grazing angles of incidence and diffraction; it is associated with the excitation of x-ray surface waves and quasiwaveguide modes, and with the study of the angular and energy dependences of the reflection spectra. An analysis of theoretical and experimental investigations in this area is carried out with the aim of determining the possibility of using these diffraction and reflection features for the study of surface layers, thin films and interfaces. The extremely asymmetric two- and multiwave diffraction schemes and the two-wave symmetric noncoplanar diffraction scheme are analyzed, as is the anomalous reflection of the x rays. The angular dependences of the anomalous reflection are calculated on the basis of a model of a nonuniform surface layer. It is shown to be possible to use the angular dependence of the reflection for the determination of the statistical characteristics of surface nonuniformities. Experiments for the determination of short range order in surface films on the basis of the analysis of the extended fine structure of reflection spectra are discussed.

CONTENTS

INTRODUCTION

Recent experiments demonstrate that x-ray optics has become a tool for the study of two-dimensional structures. Evidence for this conclusion is given by investigations of surface reconstruction of semiconductor and metal crystals, study of the phase transition in a monolayer of atoms on the surface of a single crystal, and by the study of the interface between a single crystal and a thin crystal film grown epitaxially on it. These advances stem from the use of a novel diffraction geometry based on the diffraction of waves that decay exponentially in the medium. Since the penetration depth of the wave into the medium amounts to some tens to hundreds of angstroms, such diffraction schemes are sensitive to the structure of the surface. Investigations of these diffraction schemes have led to a new type of nonuniform waves—x-ray surface waves and quasiwaveguide modes. The x-ray surface waves are strongly coupled to the boundary of the crystal; they have their maximum intensity at the crystal boundary, decay exponentially on both sides of it, and have an anomalously great propagation length along the surface. The quasiwaveguide modes occur in the case of diffraction in thin crystal films, and in this case the diffracted wave turns out to be "locked" within the film. Waves having this structure are of interest both from a general physics and an applied point of view, particularly in the generation of coherent x rays and gamma radiation in crystals.

Diffraction methods are associated with the study of long range order in crystalline systems. Studies of the fine structure of reflection spectra have made it possible to determine the structure of the short range order in amorphous film containing a few atomic layers.

 0038-5670/85/010070-15$01.80

X-ray diffraction methods are ordinarily regarded as suitable only for the investigation of bulk properties of crystals. This is because the characteristic length of formation of the diffracted wave that carries the basic information on the crystal structure lies in the range 1–100 μm. Therefore, in the investigation of thin films consisting of a few atomic layers, the intensity of the diffracted wave is extremely low. At first glance this same situation would appear to hold in x-ray absorption spectroscopy, since the optimal length of the sample for obtaining the necessary contrast is close to the absorption length, which also lies in the above-mentioned range when radiation is used whose wavelength corresponds to the K absorption edge in media of intermediate atomic number.

The thickness of the layer in which the diffracted wave is formed in the case of diffraction in reflection depends on the angle of incidence of the wave onto the crystal, and it decreases with decreasing grazing angle, i.e., the angle between the beam and the crystal face where it enters. It is natural then in studying the properties of thin films to work at grazing angles of incidence. The investigation of diffraction in this geometry poses the problem of determining the dependence of the depth of formation of the diffracted wave on the angle of incidence as the grazing angle goes to zero. Diffraction schemes which use grazing angles of incidence or of diffraction have been called extremely asymmetric diffraction schemes. A discussion of these schemes is given in section 1. In extremely asymmetric Bragg diffraction a specularly reflected wave is formed in the vacuum along with the diffracted wave, and its intensity exceeds that of the diffracted wave by several orders of magnitude. The most striking physical results have been obtained with the use of a novel arrangement, that of two-wave symmetric noncoplanar diffraction. A discussion of this scheme is given in section 2. In this case both the incident and the diffracted wave make a small angle with the surface of the crystal. The intensity of the diffracted wave is now comparable to that of the specularly reflected wave, and for certain angles of incidence the specular wave is suppressed.

A discussion of the mechanisms for the excitation of x-ray surface waves and quasiwaveguide modes and the features of their propagation are given in sections 3 and 4.

In diffraction arrangements using grazing angles of incidence, the microrelief of the crystal surface becomes important, since surface roughness causes an angular broadening of the reflected beams. In section 5 we discuss anomalous x-ray reflection effects that arise when the angle of incidence of the x rays is close to the angle of total external reflection and that are caused by the nonuniformity of the surface layer. Calculations are made of the angular dependence of the nonspecular reflection and a comparison is made of the theoretical and experimental results. It is shown that from the angular characteristics of the nonspecular reflection one can obtain information on the statistical properties of a nonuniform surface.

The determination of short range order in surface layers from an analysis of the extended fine structure of the reflection spectra is discussed in section 6.

Until recently, surface sensitive methods in x-ray optics have been based on measurements of the angle and energy dependences of the yield of secondary processes. Among these methods are, for instance, various versions of the method of x-ray standing waves.[59–63] Experimental investigations have been carried out on the fluorescent[64] and photoelectric[65] yields as a function of the x-ray angle of incidence under conditions of total external reflection. In the method of EXAFS (Extended X-ray Absorption Fine Structure) spectroscopy, the photoelectron,[66–67] Auger electron,[68] and fluorescence[69] yields have been studied as a function of the energy of the incident x rays.

In these methods the thickness of the layer that is investigated is small because of the small escape depth of the secondary particles. However, in the present paper we shall not touch upon this aspect, since, in our opinion, it is properly the subject of a separate review. In this review we shall discuss only those methods in which the properties of the surface and surface layers are studied via angular and energy spectra of elastically scattered x rays.

1. EXTREMELY ASYMMETRIC DIFFRACTION

a) Two-wave diffraction

The principal diffraction schemes in x-ray optics are the Laue (Fig. 1a) and the Bragg (Fig. 1b) diffraction geometries. The Laue diffraction geometry is that of diffraction in transmission, where the energy flux of the waves leaving the lower face of the crystal (for a nonabsorbing crystal) is equal to that of the wave incident on the crystal. In the case of Bragg diffraction there exists a range of angles of incidence within which there is total reflection of the wave incident on the crystal. An important feature of the Bragg diffraction geometry is the possibility of decreasing the angular width of the reflected beam relative to that of the incident beam and the possibility of increasing the electric field strength (for more detail see, e. g., the monograph of Ref. 1). These possibilities are realized in asymmetric diffraction, i.e., when the angle ψ between the entrance face of the crystal and the reflecting plane (the dashed line in Fig. 1) is nonzero (Fig. 1c). When

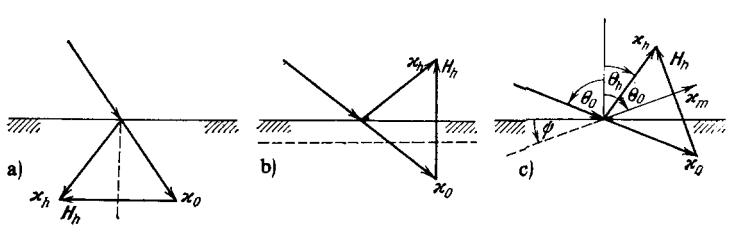

FIG. 1. Mutual arrangement of the wave vectors of the incident ($\varkappa_0$), diffracted ($\varkappa_h$), and specularly reflected ($\varkappa_m$) waves. a) Laue diffraction geometry; b) Bragg diffraction geometry; c) asymmetric diffraction.

$\theta_0 > \theta_h$ the angular width of the reflected beam decreases, as mentioned above, and when $\theta_0 < \theta_h$ the linear dimensions of the reflected beam decrease relative to those of the incident beam, and this also leads to an increase in the field strength. These properties of asymmetric diffraction have found wide application in various x-ray optics devices. If θ_0 and θ_h are close to $\pi/2$, then the corresponding diffraction schemes are termed extremely asymmetric. The case $\theta_h = \pi/2$ is intermediate between the Bragg and Laue diffraction cases. For a long time the extremely asymmetric diffraction schemes were not studied in x-ray optics. The first detailed investigations of this diffraction geometry were reported in Refs. 2–5. Later there followed a series of investigations both of the cases of x-ray[6–19] and neutron[20–22] diffraction.

Let us consider the features of extremely asymmetric diffraction. For $\theta_0 \approx \pi/2$ there appears in the vacuum along with the diffracted wave a specularly reflected wave propagating at an angle θ_0 with respect to the normal to the interface (κ_m in Fig. 1c). When the grazing angle $\eta_0 = (\pi/2) - \theta_0$ lies in the range $0 < \eta_0 < \eta_c$, where $\eta_c = \sqrt{|\chi'_0|}$ is the critical angle of total external reflection of the x rays and χ'_0 is the real part of the polarizability, the intensity of the specular wave exceeds by several orders of magnitude the intensity of the diffracted wave. This is explained principally by the difference in the exit angles of the waves.[1)] The reflection coefficients R_h and R_m are not significantly different:

$$R_h = \frac{\gamma_h}{\gamma_0}\frac{I_h}{I_0} \approx \frac{\sin 2\theta_B}{\eta_0}\frac{I_h}{I_0}, \quad R_m = \frac{I_m}{I_0},$$

where $\gamma_h = \cos\theta_h$, $\gamma_0 = \cos\theta_0$, and I_h, I_m, and I_0 are, respectively, the intensities of th diffracted, the specular, and the incident waves.

As we have noted above, for $\theta_0 > \theta_h$, the angular width $\Delta\theta_0$ of the region of total reflection of the incident beam is larger than $\Delta\theta_h$ for the reflected wave. The relation between them is given by the following expression[1]:

$$\frac{\Delta\theta_h}{\Delta\theta_0} = \frac{\sin\eta_0}{\sin\eta_h},$$

where $\eta_h = (\pi/2) - \theta_h$. Calculations which take into account the particular features of the extremely asymmetric diffraction scheme have shown that with decreasing η_0 the angular width of the diffracted wave does not go to zero, as would follow from the above formula, but approaches a limiting value.

Features that are interesting from a physical point of view appear in the case $\theta_h \approx \pi/2$. In Ref. 6 it was shown that in this case total internal reflection of the x rays is possible. As we have noted above, far from Bragg diffraction conditions the index of refraction is less than unity in the x-ray range. However, near the Bragg diffraction conditions, as a result of dynamic interaction between the refracted and diffracted waves, a strong spatial dispersion is observed, leading to the result that the modulus k_h of the wave vector of the diffracted wave can become greater than that of the wave vector in vacuum ($\varkappa = \omega/c$): $k_h = \varkappa\sqrt{\varepsilon_h} > \varkappa$, i.e., $\varepsilon_h > 1$. In the case $\theta_h = \pi/2$, when the angle of incidence is varied near the value $\theta_0 \approx 2\theta_B$ (where θ_B is the Bragg diffraction angle for the chosen family of planes) the modulus k_h can vary within the limits

$$\varkappa\left(1 - \frac{|\chi'_0|}{2}\right) \leqslant k_h \leqslant \varkappa\left(1 + \frac{|\chi'_0|}{2}\right)$$

without significant change in the intensity of the diffracted wave. Consequently, by a choice of the point of excitation on the dispersion curve, one can make the projection k_{ht} of the wave vector of the diffracted wave in the medium larger than $\varkappa$. Then from the condition of continuity of the tangential component of the wave vector at the interface we obtain $\varkappa_{hz} = \sqrt{\varkappa^2 - k_{ht}^2} = i\sqrt{k_{ht}^2 - \varkappa^2}$. Thus, the diffracted wave in the vacuum becomes nonuniform, being attenuated with distance from the interface.

A theoretical investigation of these diffraction schemes has shown that it is necessary to abandon the traditional approximations of dynamical diffraction theory. Since the refractive index in the x-ray region is only slightly different from unity, $n = 1 - \delta$, in the solution of the dispersion equation the approximation that the modulus of the refraction vector $\Delta k = \varkappa_z - k_z$ is much smaller than $\varkappa_z$ or k_z is widely used, where $\varkappa_z$ and k_z are, respectively, the projections, on the normal to the interface, of the wave vectors of the incident and refracted waves. Actually, for $\eta_c \ll \eta_0 \ll \pi/2$, we have $\Delta k \approx \varkappa\delta$, whereas $\varkappa_z = \varkappa\sin\eta_0$, and consequently $\varkappa_z \gg \Delta k$. However, when the angle η_0 approaches η_c $\varkappa_z$ approaches $\Delta k \approx \varkappa\eta_c$ and the condition $\varkappa_z \sim \Delta k > k_z$ is satisfied. There are similar changes also for the case $\eta_h \sim \eta_c$. Therefore, while in the traditional theories (see, e. g., Ref. 1) of dynamic two-wave diffraction the dispersion equation of fourth degree

$$(k_0^2 - k^2)(k_h^2 - k^2) = \varkappa^4 (\mathbf{e}_0\mathbf{e}_h)^2 \chi_{\bar{h}}\chi_h, \tag{1.1}$$

where $k = \varkappa\sqrt{\varepsilon} = \varkappa\sqrt{1 + \chi_0}$, χ_h is a Fourier component of the polarizability of the crystal, and $\mathbf{e}_0$ and $\mathbf{e}_h$ are the unit vectors of the polarization of the waves, is replaced by a second degree equation

$$(k_0 - k)(k_h - k) = \frac{\varkappa^2}{4}(\mathbf{e}_0\mathbf{e}_h)^2 \chi_{\bar{h}}\chi_h, \tag{1.2}$$

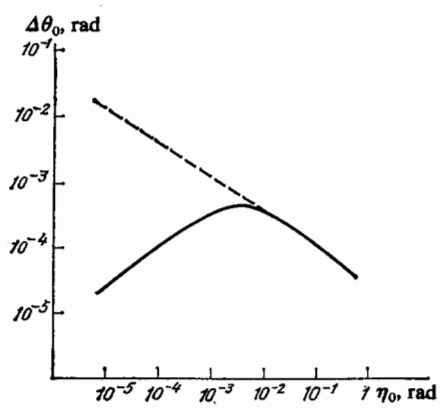

FIG. 2. Width $\Delta\theta_0$ of reflection curve as a function of the angle of incidence η_0 (Ref. 7). Solid curve: theory of extremely asymmetric diffraction. Dashed curve: calculated from a dispersion equation of the form (1.2).

[1)] In the Laue diffraction geometry the intensity of the transmitted wave increases.

in the case of extremely asymmetric diffraction this replacement is not admissible. The solution of (1.1) cannot always be given in a compact analytical form, which makes the analysis of this diffraction geometry difficult. Various approximate solutions of Eq. (1.1) have been obtained.[7,20] Figure 2 shows the dependence of the angular width $\Delta\theta_0$ of the reflectance curve on the grazing angle η_0 for calculations with Eq. (1.1) (the solid curve) and Eq. (1.2) (the dashed curve). It can be seen that these two curves diverge significantly for small η_0.

b) Multiwave diffraction

In multiwave diffraction schemes a single one of the waves taking part in the diffraction or various combinations of the waves can make a small angle with the surface of the crystal, and among these combinations is included the set of all the waves, when all the reflecting planes are perpendicular to the entrance surface of the crystal. In crystals oriented so that the entrance surface coincides with one of the crystal planes, extremely asymmetric diffraction schemes are as a rule, not two-wave, but multiwave. Actually, in oriented crystals the diffracted wave (for $\theta_h \approx \pi/2$) or the refracted wave (for $\theta_0 \approx \pi/2$) propagates almost parallel to one of the crystal planes. Therefore, if in the diffraction there is a plane that makes an angle ψ with the surface of the crystal, then in the diffraction there will also be a plane making an angle $-\psi$ with the surface (Fig. 3a).

Let us now discuss the features of the extremely asymmetrical multiwave diffraction scheme. In Ref. 23 the diffraction of Cu K β radiation by the (311) planes of single crystal silicon was studied for the case where the entrance surface coincided with the (100) plane. In this case we have three-wave diffraction (311)/($\bar{3}$11)/(600) for a small angle of incidence (scheme 1) or (311)/(600)/($\bar{3}$11) for a large angle of incidence (scheme 2). Figures 3b and 3c show the form of the angular dependences of the intensities of the waves in vacuum. Figure 3b (scheme 1) shows the intensity I_m of the specularly reflected wave and the intensity I_{311} of the diffracted wave as a function of the grazing angle η_0 for various values of the angle $\delta\varphi = \varphi - \varphi_0$ in the plane of the entrance surface, where φ_0 corresponds to the Laue three-wave point. Figure 3c (scheme 2) shows the intensities I_{311} and I_{600} of the diffracted waves as a function of the angle of incidence $\delta\theta = \eta_0 - 2\theta_B$

Thus, for grazing angles of incidence the angular dependence of the intensity of the specularly reflected wave deviates only insignificantly from the corresponding one-wave curve. The angular width of the diffracted wave in vacuum $[I_{311}(\eta_0)]$ increases substantially and becomes comparable to η_c. The intensity of the diffracted wave is several orders of magnitude lower than that of the specularly reflected wave. We note that just as in the case of two-wave diffraction, the coefficient of reflection R_h and of specular reflection R_m are not significantly different.

At large angles of incidence the main features are the possibility of internal reflection and of excitation of x-ray surface waves (see section 3).

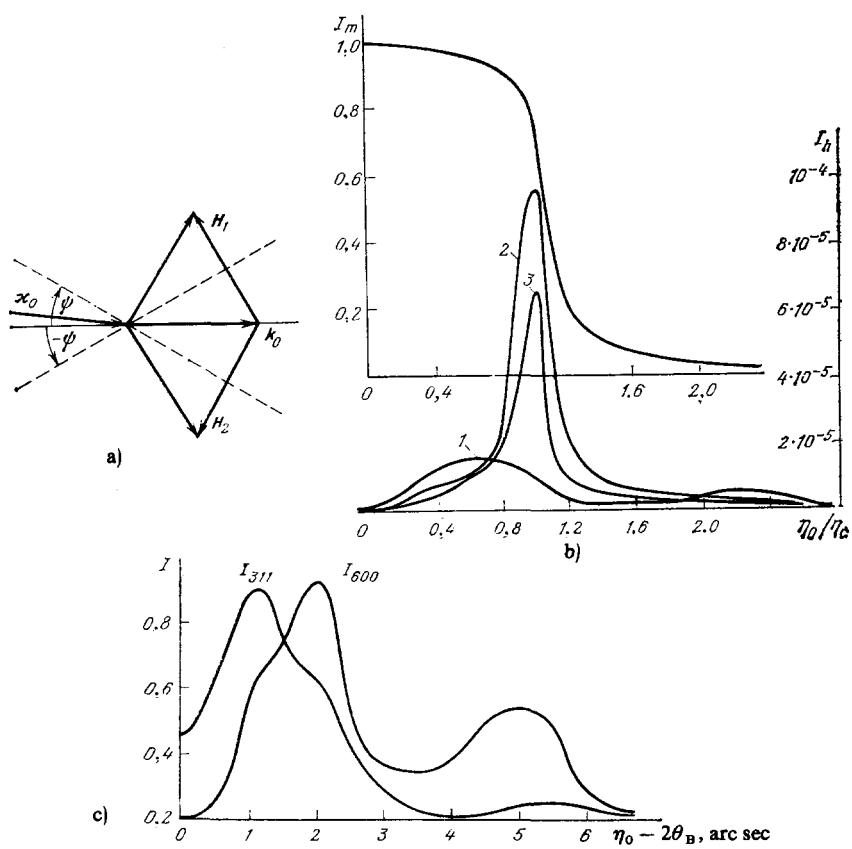

FIG. 3. a) Geometry of extremely asymmetric diffraction in oriented crystals; b) I_m and I_h, intensities of specularly reflected and diffracted waves, respectively, as functions of grazing angle η_0 of the incident wave (scheme 1). Curves 1–3 correspond to deviations $\Delta\varphi$ = 1) 0, 2) 33″, 3) 5.6′; c) intensities I_{311} and I_{600} of diffracted waves as functions of the angle of incidence (scheme 2).

An interesting feature of coplanar three-wave diffraction is that the degree of the dispersion equation in this case is reduced relative to the case of two-wave extremely asymmetric diffraction. Actually, now the dispersion curve becomes symmetric about the interface and its equation becomes a third degree equation in k_z^2. A third degree dispersion equation is a good approximation also for weak noncoplanarity, where the Laue point moves off the plane formed by the reciprocal lattice vectors of the reflecting planes.

2. TWO-WAVE SYMMETRIC NONCOPLANAR DIFFRACTION

a) General characteristics of the diffraction scheme

When the reflecting planes are perpendicular to the entrance surface of the crystal, then a situation is possible where both the angles η_0 and η_h approach close to η_c simultaneously. This diffraction scheme can be called noncoplanar two-wave diffraction, since, in contrast to usual two-wave diffraction schemes,[1] here the incident, the refracted, and the diffracted waves do not lie in a single plane. A calculation of the amplitudes of the specularly reflected and the diffracted waves in vacuum for this diffraction geometry was first carried out in Ref. 24, where it was noted that in this geometry instead of a single critical angle of reflection, there are several.

The geometry of symmetrical noncoplanar two-wave diffraction was obtained experimentally in Ref. 25. These authors studied the structure of aluminum films grown by molecular beam epitaxy on GaAs crystals having a 2 μm thick surface layer produced by molecular beam autoepitaxy. The variation of the aluminum lattice constant in the planes parallel to the interface was studied as a function of the distance from the interface. For this purpose the authors used diffraction by aluminum planes perpendicular to the entrance surface in films of various thicknesses from 75 to 2000 Å. The grazing angle of the x-ray beam was chosen such that $\eta_c^{(Al)} < \eta_0 < \eta_c^{(GaAs)}$, i.e., the wave was incident on the crystal at an angle greater than the critical angle of reflection at the film and less than the critical angle of total reflection from the substrate. This condition led to an increase in the intensity of the incident wave compared to that in transmission experiments. In Table I, which is reproduced from Ref. 25, are shown the values of the measured shift $|\varkappa_h - \varkappa_m|$ in units of $2\pi/a_0$, for various film thicknesses for the (220) reflection (the plane of the crystal was the (00l) plane), where $\varkappa_h$ is the wave vector of the diffracted wave, $\varkappa_m$ is that of the specularly reflected wave, and a_0 is the lattice constant of the GaAs substrate.

In Refs. 26–28 experiments were carried out on the use of noncoplanar two-wave diffraction geometry for the study of crystal surfaces. In Ref. 26 the surface structure of single crystal germanium and the formation of the (2×1) structure of the Ge (001) surface were studied. It was shown that the surface reconstruction involves not only the first layer. In Ref. 27 the solid-liquid phase transition in a monolayer of Pb on the Cu (110) surface was studied. In this investigation synchrotron radiation was used as the source of x rays. In Ref. 28 the formation of the (2×1) structure on the Au (110) surface was studied.

These experimental investigations showed that this method has a wide application in the study of two-dimensional phase transitions, the growth of thin films, and the behavior of clusters on crystal surfaces.

The features of the symmetric noncoplanar two-wave diffraction geometry that are associated with the possibility of excitation of x-ray surface waves have been studied in Refs. 23 and 29. The theoretical and experimental investigation of this diffraction geometry were the subjects of Refs. 30–34.

b) Features of the diffraction geometry

In this section we derive, on the basis of the formulas of Ref. 23, several simple relations that characterize the ratio of the intensities of the specular and diffracted waves in vacuum and the magnitude of the linear displacement of the reflected beam relative to the incident beam. There is always a displacement of the reflected beam relative to the incident beam when the Fresnel coefficients are complex, and in this case the displacement can serve as a measure of the degree to which the diffraction is dynamic.

Figure 4 shows the diffraction arrangement and a cross-section of the dispersion surface. This diffraction geometry permits an exact solution of the Fourth-degree dispersion equation (1.1). The solution has the form

$$k_{0i}^2 = \varkappa^2\left(\varepsilon - \frac{\alpha}{2} \pm \sqrt{\frac{\alpha^2}{4} + (e_0, e_h)^2 \chi_{\bar{h}}\chi_h}\right) = \varkappa^2 \varepsilon_{0i}, \qquad (2.1)$$

where $\varepsilon = 1 + \chi_0$ and $\alpha = 2\delta\varphi \cdot \sin 2\varphi_0 \cdot \sin^2\theta_0$ is the deviation parameter. Figure 4b illustrates the existence of two critical angles

$$\eta_{ci} = \sqrt{1 - \varepsilon_{0i}}. \qquad (2.2)$$

One of the critical angles corresponding to dispersion branch 1 in Fig. 4b is associated with a Borrmann mode, which has antinodes of the field in the space between the planes and nodes at the atom planes. The second critical angle is associated with an anti-Borrmann mode, which has the antinodes of the field at the atom planes. The difference between η_{c1} and η_{c2} is substantial and reaches several minutes of arc. For example, for the (220) reflection in silicon of Cu Kα radiation for zero deviation parameter, $\Delta\varphi = 0$, we

TABLE I.

Thickness of aluminum film in atomic layers	1000	415	100	35
Shift of Al (220)	—	0.0025	0.005	0.0128

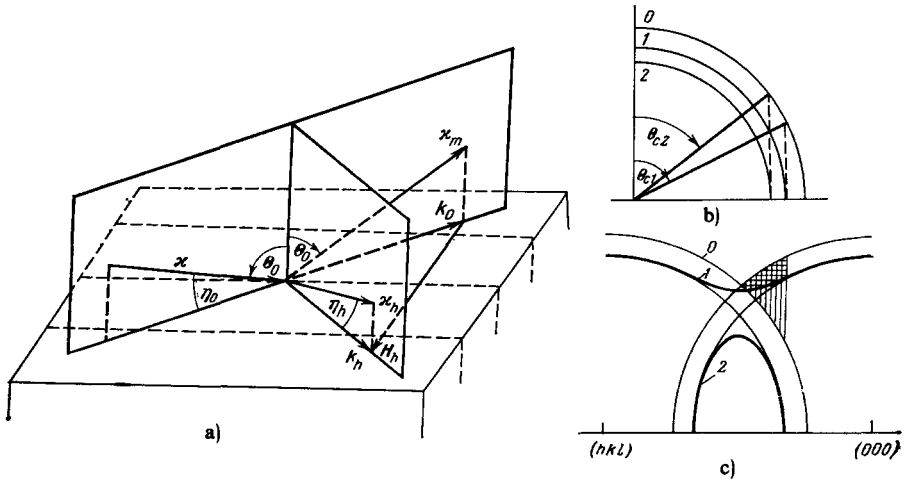

FIG. 4. a) Two-wave noncoplanar diffraction geometry. Cross sections of dispersion surface: b) formed by the plane perpendicular to the reciprocal lattice vector $\mathbf{H}_h$ and passing through its middle; c) formed by exit face of the crystal.

have $\eta_{c1} = 8.4'$ and $\eta_{c2} = 16.9'$. Thus, if the grazing angle of the incident beam lies in the range $\eta_{c1} < \eta_0 < \eta_{c2}$, then one can separate in space those beams that correspond to the Borrmann and anti-Borrmann modes. The waves that correspond to the anti-Borrmann mode will emerge into the vacuum through the entrance surface of the crystal along the direction of the specularly reflected wave, while the waves corresponding to the Borrmann mode can emerge through the side or the lower surface of the crystal. The waves corresponding to the various states of polarization can be separated in exactly the same way. For example, for the case considered above, but for polarization in the plane of diffraction, we obtain $\eta_{c1}^{(\pi)} = 10.2'$ and $\eta_{c2}^{(\pi)} = 15.9'$.

The form of the dependence of the intensities of the specularly reflected and the diffracted waves in vacuum on the angle of incidence and on the deviation parameter is shown in Fig. 5.

The expressions for $\mathscr{E}_m$ the amplitude of the specularly reflected wave and $\mathscr{E}_h$, the amplitude of the wave in vacuum have the simplest form for $\alpha = 0$.[2)]

$$r_m^{(s)} = \frac{\mathscr{E}_m}{\mathscr{E}} = \frac{r_{1s}+r_{2s}}{2}, \quad r_h^{(s)} = \frac{\mathscr{E}_h}{\mathscr{E}} = \frac{r_{1s}+r_{2s}}{2}, \tag{2.3}$$

where $\mathscr{E}$ is the amplitude of the incident wave and r_{is} is the Fresnel coefficient for each sheet of the dispersion surface (the parameter s defines the polarization state of the incident wave: $s = \perp$ and $s = \parallel$ mean, respectively, perpendicular and parallel to the plane of incidence):

$$r_{i\perp} = \frac{\cos\theta_0 - \sqrt{\varepsilon_{0i}^{(\pi)} - \sin^2\theta_0}}{\cos\theta_0 + \sqrt{\varepsilon_{0i}^{(\pi)} - \sin^2\theta_0}},$$

$$r_{i\parallel} = \frac{\varepsilon_{0i}^{(\sigma)}\cos\theta_0 - \sqrt{\varepsilon_{0i}^{(\sigma)} - \sin^2\theta_0}}{\varepsilon_{0i}^{(\sigma)}\cos\theta_0 + \sqrt{\varepsilon_{0i}^{(\sigma)} - \sin^2\theta_0}}. \tag{2.4}$$

For $\eta_0 \leqslant \eta_{c1}$ formula (2.3) has the form

$$\begin{aligned} r_m^{(s)} &= \cos(\varphi_1^{(s)} - \varphi_2^{(s)})\exp[-i(\varphi_1^{(s)} + \varphi_2^{(s)})], \\ r_h^{(s)} &= -i\sin(\varphi_1^{(s)} - \varphi_2^{(s)})\exp[-i(\varphi_1^{(s)} + \varphi_2^{(s)})], \end{aligned} \tag{2.5}$$

where

$$\varphi_i^{(\perp)} = \operatorname{arctg}\left(\sqrt{\sin^2\theta_0 - \varepsilon_{0i}^{(\pi)}}\,(\cos\theta_0)^{-1}\right),$$

$$\varphi_i^{(\parallel)} = \operatorname{arctg}\left(\sqrt{\sin^2\theta_0 - \varepsilon_{0i}^{(\sigma)}}\,(\varepsilon_{0i}^{(\sigma)}\cos\theta_0)^{-1}\right).$$

In particular, for $\theta_0 = \theta_{c1}$ the coefficients $|r_h|^2$ and $|r_m|^2$ have the form

$$|r_h|^2 = \frac{2|\chi_h|}{|\chi_0|+|\chi_h|}, \quad |r_m|^2 = \frac{|\chi_0|-|\chi_h|}{|\chi_0|+|\chi_h|}. \tag{2.6}$$

Thus, for reflection of CuKα radiation from the (220) plane of silicon[3)] we have

$$|r_h|^2 = 0{,}754, \quad |r_m|^2 = 0{,}246.$$

Expression (2.6) refers to the case $\alpha = 0$, where the grazing angles η_0 and η_h are equal and therefore $|r_m|^2 + |r_h|^2 = 1$. For $\alpha > 0$ the angle $\eta_h < \eta_0$ so that $|r_h|^2$ can take on values greater than unity.

Let us now determine the linear displacement of the reflected beam relative to the incident beam. If the size of the slit in the diaphragm that delimits the beam incident on the crystal satisfies the condition $\varkappa l\cos\theta_0 \gg 1$, then the displacement of the specularly reflected wave relative to the incident wave is given by the formula

$$l_s = -\frac{1}{\varkappa}\frac{\partial\varphi^{(s)}}{\partial\sin\theta}\Big|_{\theta=\theta_0}. \tag{2.7}$$

[2)]The general expression for the coefficients r_m and r_h when the polarization vector of the incident radiation is perpendicular to the plane of incidence has the form

$$r_m = \frac{(\varepsilon_{01}-\varepsilon)(\varkappa_z+k_{z2})(\varkappa_{hz}+k_{z1}) - (\varepsilon_{02}-\varepsilon)(\varkappa_z-k_{z1})(\varkappa_{hz}+k_{z2})}{(\varepsilon_{01}-\varepsilon)(\varkappa_z+k_{z2})(\varkappa_{hz}+k_{z1}) - (\varepsilon_{02}-\varepsilon)(\varkappa_z+k_{z1})(\varkappa_{hz}+k_{z2})},$$

$$r_h = \frac{2(\varepsilon_0\varepsilon_h)\chi_h\varkappa_z(k_{z1}-k_{z2})}{(\varepsilon_{01}-\varepsilon)(\varkappa_z+k_{z2})(\varkappa_{hz}+k_{z1}) - (\varepsilon_{02}-\varepsilon)(\varkappa_z+k_{z1})(\varkappa_{hz}+k_{z2})},$$

where $\varkappa_z$ is the projection of the wave vector of the incident wave on the normal to the interface, $\varkappa_{hz} = (\varkappa_z^2 - \varkappa^2\alpha)^{1/2}$ is the same for the vacuum diffracted wave, and k_{z1} and k_{z2} are the same for the waves in the medium. From these expressions it follows, in particular, that in a nonabsorbing crystal, in the region of excitation points that correspond to purely imaginary values of k_{z1}, k_{z2}, and $\varkappa_{hz}$, the coefficient $|r_m| = 1$ (for more detail, see section 4).

[3)]For γ-ray and neutron diffraction, where $\chi_0 \approx \chi_h$ is possible, there is a strong supression of the specular wave.

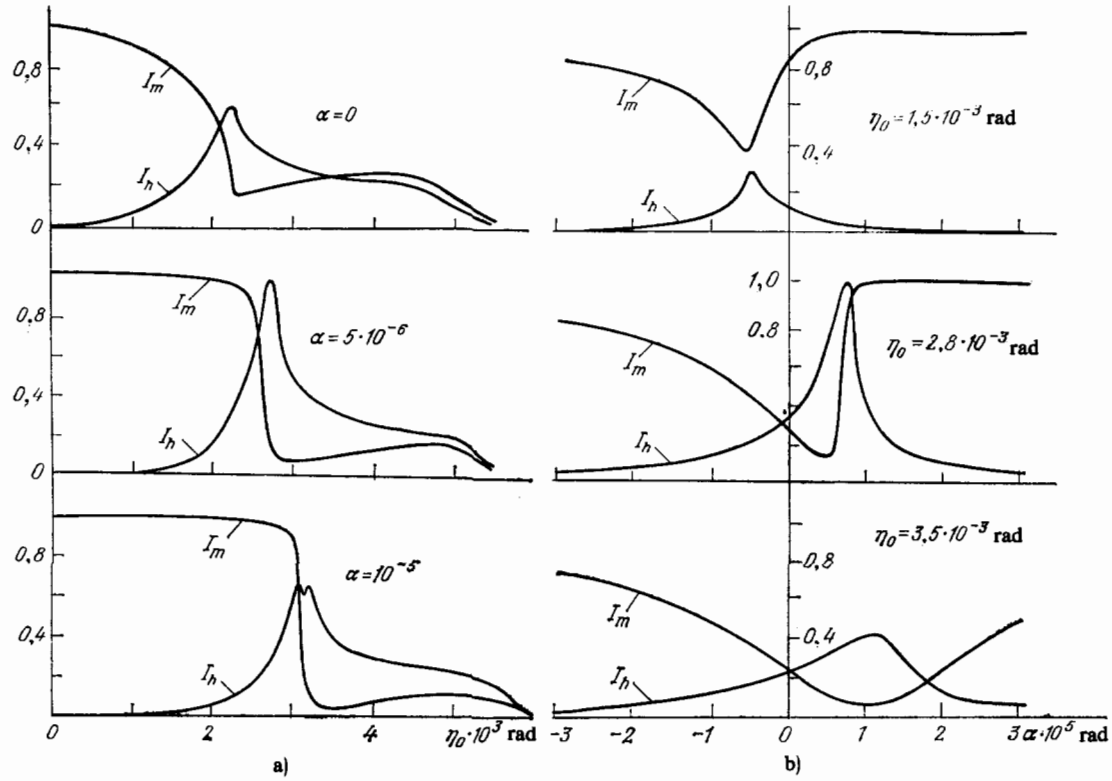

FIG. 5. a) Intensity $I_m = |\mathscr{E}_m|^2$ of specular wave and $I_h = \mathscr{E}_h|^2$ of vacuum diffracted wave as functions of grazing angle, and b) as functions of the deviation parameter.

For $\alpha = 0$ we obtain from (2.3)–(2.5)

$$l_\perp = \frac{\lambda}{2\pi} \sum_{i=1}^{2} \frac{\operatorname{tg}\theta_0}{\sqrt{\sin^2\theta_0 - \varepsilon_{0i}^{(\pi)}}},$$

$$l_\parallel = \frac{\lambda}{2\pi} \sum_{i=1}^{2} \frac{\varepsilon_{0i}^{(\sigma)}}{\varepsilon_{0i}^{(\sigma)} + (1+\varepsilon_{0i}^{(\sigma)})\sin^2\theta_0} \frac{\operatorname{tg}\theta_0}{\sqrt{\sin^2\theta_0 - \varepsilon_{0i}^{(\sigma)}}}.$$

The displacement is a maximum when the condition $\sin^2\theta_0 = \varepsilon_{01}$ is satisfied. In this case $l_\parallel$, for example, has the form

$$l_\parallel = \frac{\lambda}{\pi} \sqrt{\frac{\varepsilon_{01}'}{2(1-\varepsilon_{01}')\varepsilon_{01}''}}.$$

The ratio of this quantity to the maximum displacement $l_\parallel^{(OB)}$ far from the Bragg condition has the form

$$\frac{l_\parallel^{(B)}}{l_\parallel^{(OB)}} = \frac{1}{2}\left[\left(1 - \frac{|\chi_h'|}{|\chi_0'|}\right)\left(1 - \frac{|\chi_h''|}{|\chi_0''|}\right)\right]^{-1/2}.$$

Thus, the maximum displacement of the reflected wave under diffraction conditions exceeds the maximum value of $l_\parallel^{(OB)}$ by more than an order of magnitude for strong reflections. This is due to two reasons: 1) the anomalous penetration depth of the Borrmann wave into the crystal, and 2) the change in the critical angle for total external reflection.

3. X-RAY SURFACE WAVES

Previously we have found two forms of nonuniform x-ray waves. Far from the Bragg conditions and for an angle of incidence θ_0 of the wave on the crystal greater than the critical angle θ_c there is total external reflection, and nonuniform waves that decay exponentially with distance from the interface propagate in the medium. On the other hand, in the case of extremely asymmetric diffraction, as was shown in section 1, the phenomenon of total internal reflection can occur, with the appearance of a nonuniform wave in the vacuum. It turns out that these two types of nonuniform waves do not exhaust all the possibilities. In Ref. 29 it was shown that the excitation of waves with a more complicated structure is possible; these are waves that have a maximum at the interface and decay exponentially on both sides of it (i.e., the wave propagates along the interface and decays exponentially on both sides of it). Waves having this structure have been called[29] x-ray surface waves.

Let us discuss the mechanism of the excitation of x-ray surface waves, using by way of example two-wave noncoplanar diffraction. A cross section of the dispersion surface and the diffraction geometry are shown in Fig. 4. In the area with the vertical crosshatching in Fig. 4c the projection of the wave vector of the diffracted wave on the interface is larger than the magnitude $\varkappa = \omega/c$ of the wave vector in vacuum, i.e., the condition for total internal reflection of the diffracted wave is satisfied. In the region with the horizontal crosshatching the condition for total external reflection is satisfied; here all the waves that propagate in the medium are nonuniform. Thus, in the region of excitation points where there is the double crosshatching the conditions for total internal reflection and for total external reflection are simultaneously satisfied. In this case the diffracted wave travels

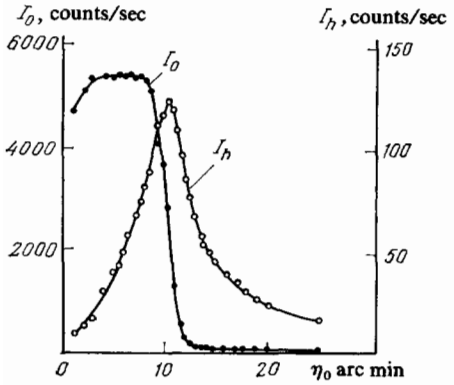

FIG. 6. Experimentally determined[23] intensity I_0 of specular and I_h of vacuum diffracted wave as functions of grazing angle η_0 for sapphire crystal, CuKα radiation.

along the surface of the crystal, has its maximum intensity there, and decays exponentially on both sides of it.

In Ref. 23 the two-wave noncoplanar geometry was realized with the use of the reflection of CuKα radiation from the $(10\bar{1}1)$ plane of sapphire. Figure 6 shows the experimentally determined dependence of the intensities I_0 of the specularly reflected wave and I_h of the diffracted wave in vacuum on the grazing angle η_0. The angular width of the incident beam in the plane parallel to the entrance surface was much greater than the corresponding width in the region of Bragg reflection, and this result accounts for the experimentally obtained relation between the intensities I_m and I_h. The dependences that were obtained agree qualitatively with the corresponding theoretical calculations (see Fig. 5). It is necessary only to note that because of the difference observed in the curves in Fig. 6, it is necessary to make a comparison of the curves integrated over α. Figure 7 shows

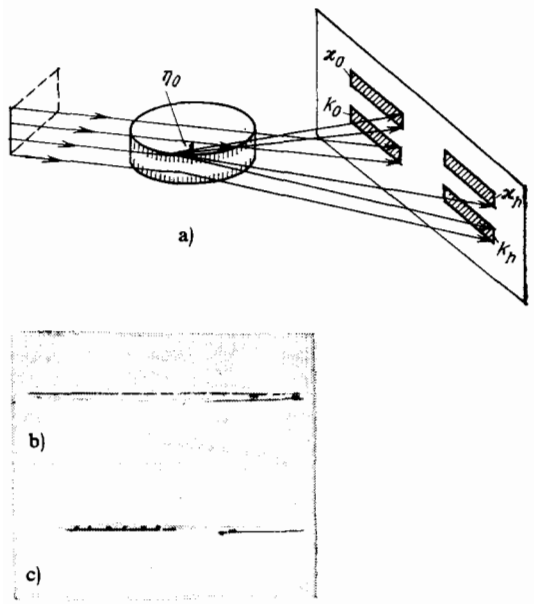

FIG. 7. a) Experimental arrangement; and diffraction pattern for b) positive, and c) negative deviation from exact Bragg condition.[23]

the experimental arrangement and the form of the angular dependence of the diffracted wave intensity on the azimuthal deviation of the incident wave. In view of the discrepancy in angle noted above, the amount of deviation was estimated from the decrease in intensity of the diffracted wave by one-half relative to its maximum value for a given angle of incidence θ_0. Figures 7b and 7c correspond, respectively, to negative and positive deviation. It can be seen that for positive deviation the intensity maximum of the diffracted wave shifts towards the surface of the crystal. This circumstance undoubtedly indicates that the mechanism of the formation of the diffracted wave is associated with dynamic diffraction effects.

In Ref. 23 it was shown that x-ray surface waves also arise in similar multiwave diffraction schemes, for instance in noncoplanar three-wave diffraction (all the reflecting planes are perpendicular to the entrance surface), as well as in multiwave coplanar diffraction schemes. An example is the diffraction scheme discussed above, in which CuKβ radiation is diffracted in silicon crystals by the $(311)/(600)/(\bar{3}1\bar{1})$ planes and the entrance surface coincides with the (100) plane. The main difference between this diffraction scheme and the noncoplanar two-wave scheme is that the attenuation of the wave in the medium in this case is due to the fact that the surface wave is excited within the Bragg reflection region. As a result, the depth of penetration of the wave into the medium is considerably enhanced.

In conclusion to this section we shall estimate how critical, from the point of view of surface wave excitation, the noncolinear two-wave diffraction scheme is to deviations from exact perpendicularity of the reflecting planes to the surface of the crystal. Let ψ be the angle between the reciprocal lattice vector and the plane of the crystal. Then the relation between the exit angle η_h of the diffracted wave into the vacuum, the grazing angle η_0 the incident wave, and the deviation parameter α has the form

$$\eta_h = \sqrt{\eta_0^2 - \alpha + 2\psi^2 \sin^2\theta_B}.$$

If the reflecting planes are exactly perpendicular to the entrance surface of the crystal, then the region of surface wave excitation is determined by the condition

$$\alpha > \eta_0^2.$$

If $\psi \neq 0$ then this condition takes the form

$$\alpha > \eta_0^2 + 2\psi^2 \sin^2\theta_B.$$

Thus, for $\eta_0 > \psi \sin\theta_B$ the region of surface wave excitation is practically unchanged. This condition can easily be fulfilled even for mechanically prepared surfaces.

4. QUASIWAVEGUIDE MODES

Since for x rays the vacuum is an optically more dense medium than matter, waveguide propagation of x rays could exist in an air gap between two plates. However, the main part of the energy of the x-ray wave will in this case be concentrated in the vacuum, whereas in the investigation of the structure of matter it is desirable to increase the interaction of the field and the medium. Waveguide modes can also be excited in less dense layers sandwiched between more dense

layers. Quite frequently, however, the problems one encounters involves layers that are deposited on a substrate, i.e., layers, one of whose interfaces is with the vacuum. If these layers are crystalline, then the use of dynamic total internal reflection[4)] permits the excitation of quasiwaveguide modes, where the diffracted wave is locked within the layer, while undergoing total reflection both at the layer-vacuum and the layer-substrate interfaces. Such quasiwaveguide modes and the possibility of their application in the generation of coherent Mössbauer radiation have been studied in Ref. 56.

To understand and explain the conditions for the excitation of the quasiwaveguide modes we shall return to the two-wave noncoplanar diffraction scheme. In the excitation region with single crosshatching in Fig. 4c, the condition of total reflection is satisfied both at the layer-vacuum interface: $|k_{ht}| > \varkappa$, where k_{ht} is the projection of the wave vector on the interface, and, of course, at the layer-substrate interface: $|k_{ht}| > \varkappa n_s$, where n_s is the refractive index of the substrate. The interior sheet of the dispersion surface corresponds to waves that decay exponentially within the layer, while the outer sheet (with an anomalously small absorption coefficient) will correspond to uniform plane waves having projections k_{zi} of the wave vectors on the normal to the interface that is determined by the intersection of the normal and the dispersion surface. For a layer of thickness d, those points will be selected for which

$$(k_{z1} - k_{z2})\, d - \phi_1 - \phi_2 = \pi n,$$

where ϕ_1 and ϕ_2 are the phases of the coefficients of reflection from the boundaries of the layer.

The region of excitation of x-ray surface waves corresponds in a certain sense to the zero waveguide mode in an infinitely thick layer.

The interest in the quasiwaveguide modes from the point of view of generating coherent Mössbauer radiation lies in the possibility of increasing the amplification factor $G = \exp[(\mu_+ - \mu_-) \cdot L]$, where μ_+ and μ_- are the coefficients of amplification and absorption, and $\tau = L/c$ is the interaction time of the resonance radiation with the medium. The decrease in the factor $(\mu_+ - \mu_-)$ in the exponent, due to the fact that the region of excitation of the quasiwaveguide and surface modes lies at the edges of the reflection maximum can be substantially compensated by the increase in L, the effective length of the interaction of the field with the medium. A planar layer on a crystal surface is a natural form for the active region in the application of laser annealing to the reconstruction of a crystal lattice that has been damaged by intense pumping of nuclear transitions.[57,58]

5. ANOMALOUS REFLECTION OF X RAYS

In this section we shall discuss the features of the angular dependence of the reflection of x rays incident on a crystal at angles that are close to the critical angle for total external reflection. Total external reflection has been finding ever wider application in the investigation of surface layers of various materials. The problems of the use of total external reflection in x-ray optical systems such as x-ray microscopes and telescopes of the reflection type, collimation devices, and so forth, and the use of total external reflection for the determination of surface quality are addressed in the review of Ref. 35. While not dwelling at length on these aspects, we shall discuss here two effects: 1) the anomalous reflection of x rays incident on a crystal at an angle less[36] than the critical angle θ_c, and 2) the anomalous reflection of x rays incident on a crystal at an angle greater[37] than the critical angle θ_c.

a) Anomalous reflection for angles of incidence less than θ_c, the critical angle for total external reflection

The first effect was observed twenty years ago; it has been studied many times since then[38–42] and the investigations have continued up to the present time.[43–45] A number of models have been proposed to explain the phenomenon (for more detail, see Ref. 35); however there have been few attempts to calculate theoretically the angular dependence.[41–42]

The essence of the effect is the following: when a beam of x rays is incident on a crystal at a grazing angle that is 2–3 times greater than the critical angle, then, besides the specularly reflected wave, an additional peak in the angular distribution of reflected rays appears at an angle, somewhat less than the angle of incidence, with respect to the crystal surface (Fig. 8). Such a structure is observed in the reflected field for various materials and it exhibits the following regularities: 1) the angle η_a is independent of the angle of incidence η_0 and the ratio of η_a to η_c, the critical angle for total external reflection, is[45] $\eta_a/\eta_c = 0.91 \pm 0.11$; 2) the angle η_a varies approximately proportionately to the wavelength; 3) The integrated intensity I of the anomalously reflected beam in the first place decreases with increasing grazing angle η_0 and in the second place depends on the imaginary part of the refractive index; 4) a study of the anomalous reflection from

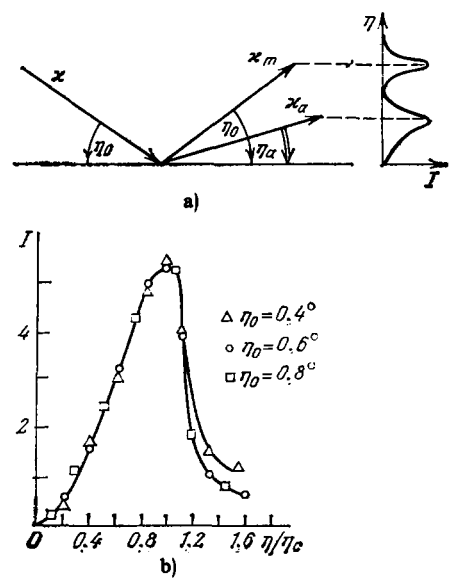

FIG. 8. a) Anomalous reflection effect; b) form of angular distribution of anomalous reflection for various angles of incidence (K8 glass).[45]

[4)]We use the term "dynamic total internal reflection" to emphasize that we are dealing with total internal reflection resulting from dynamic diffraction.

samples of K8 glass, prepared having 8th to 14th class roughness, has shown[45] that first, the maximum intensity of the anomalous reflection is observed for the 11–12 class of roughness and, second, the magnitude depends on the class of surface roughness while the angular profile is practically independent of it.

These regularities that we have listed allow us to conclude that the angular position of the peak of the anomalous reflection is determined by the refractive index of the given material, and mainly by the magnitude of the refractive index in the surface layer of the material.

b) Anomalous reflection for angles of incidence greater than θ_c the critical angle for total external reflection

In Ref. 37 during the study of total external reflection of x rays from ion bombarded silicon crystals the following effects were observed: 1) the angular width of the reflected beam was considerably greater than that of the incident beam; 2) In the angular dependence of the reflection an additional peak appeared which corresponded to waves traveling along the crystal surface; 3) the ratio of the intensity of the specular peak to that of the secondary peak depended on the position of the illuminated region (Fig. 9). For illumination at the edge of the sample only the secondary peak is observed, and as the illuminated region is moved away from the edge of the sample the intensity of the specular peak increases and that of the secondary peak falls off; 4) the relation of the intensities of the two peaks depended on the dose of ions to the crystal[46]; 5) in the case of reflection from nonirradiated crystals and amorphous media the secondary peak was not observed, and the angular width of the specularly reflected beam decreased.

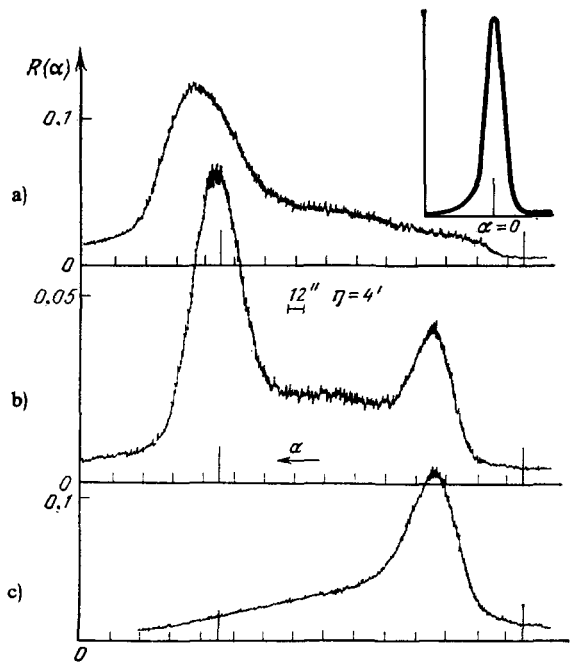

FIG. 9. Dependence[37] of angular distribution of reflection on position of illuminated region. Distrance between beam edge and crystal edge: a) 30 mm; b) 21 mm; c) 4 mm. The inset shows the shape of the beam in the absence of the crystal.

c) Theory of reflection of x rays from media with a nonuniform surface layer

The review of the experimental data presented above shows that the principal mechanism for the anomalous reflection is evidently small-angle scattering by nonuniformities in the surface layer.

In this section, on the basis of a model of a nonuniform transition layer we calculate the main characteristics of the angular dependence of the reflection.

Let us consider the reflection of x rays from a sample with a nonuniform surface layer. We shall not specify the form of the nonuniformity. It may be due either to surface roughness or to the presence of radiation defects in the layer next to the surface, or to other such factors. Taking into account the electron density in the nonuniform layer by the random fluctuation of the position vector $\mathbf{r}$, we can represent the dielectric permittivity in the form

$$\varepsilon(\mathbf{r}) = \varepsilon_0(z) + \delta\varepsilon(\mathbf{r}), \tag{5.1}$$

where $\varepsilon_0(z) = \langle\varepsilon(\mathbf{r})\rangle$ is the dielectric permittivity averaged over the density fluctuations; the z axis points down into the sample, perpendicular to the surface, and $\delta\varepsilon(\mathbf{r})$ is the fluctuation in the dielectric permittivity. We write the amplitude of the field in the form of a regular component $E_0(\mathbf{r})$ that satisfies the equation

$$\Delta E_0(\mathbf{r}) + \varkappa^2\varepsilon_0(z)\,E_0(\mathbf{r}) = 0, \tag{5.2}$$

and a component $\delta\varepsilon(\mathbf{r})$ that is scattered by the fluctuations and obeys the equation

$$\Delta E_1(\mathbf{r}) + \varkappa^2\varepsilon_0(z)\,E_1(\mathbf{r}) = -\varkappa^2\delta\varepsilon(\mathbf{r})\,E_0(\mathbf{r}). \tag{5.3}$$

Since in the absence of diffraction polarization effects are unimportant, we can limit the treatment to scalar amplitudes.

Let us assume that there is incident onto the crystal a plane wave with wave vector

$$\varkappa_0 = \{\varkappa_{||},\ \varkappa_z\},$$

where $|\varkappa_{||}| = \varkappa\sin\theta_0$, $\varkappa = \omega/c$, and θ_0 is the angle of incidence with respect to the normal to the interface. Then the field $E_0(\mathbf{r})$ can be written in the form

$$E_0(\mathbf{r}) = E_0(z)\exp(i\varkappa_{||}\rho),$$

where $E_0(z)$ satisfies the equation

$$\frac{d^2E_0}{dz^2} + (\varkappa^2\varepsilon_0 - \varkappa_{||}^2)\,E_0 = 0. \tag{5.4}$$

As linearly independent solutions of Eq. (5.4) we can choose solutions with the following asymptotic forms:

$$u(z) = \begin{cases} e^{i\varkappa_z z} + re^{-i\varkappa_z z}, & z\to-\infty, \\ te^{ik_z z}, & z\to\infty; \end{cases}$$

$$v(z) = \begin{cases} t_1 e^{-i\varkappa_z z}, & z\to-\infty, \\ e^{-ik_z z} + r_1 e^{ik_z z}, & z\to\infty, \end{cases} \tag{5.5}$$

where $k_z = \varkappa\sqrt{\varepsilon - \sin^2\theta}$, ε is the bulk value of the dielectric permittivity, r and t are, respectively, the amplitudes of the reflected and refracted waves for the case where the wave is incident onto the interface from the vacuum to the medium, and r_1 and t_1 are those same quantities when the wave is

incident onto the interface from the medium to the vacuum. Using (5.5) we can write Eq. (5.3) in the form

$$E_1(\mathbf{r}) = -\int d\mathbf{k}_{\parallel} \frac{e^{i\mathbf{k}_{\parallel}\rho}}{W}\Big[u(z)\int_{-\infty}^{z} F(\mathbf{s}, z')\,v(z')\,dz' + v(z)\int_{z}^{\infty} F(\mathbf{s}, z')\,u(z')\,dz'\Big], \quad (5.6)$$

where

$$F(\mathbf{s}, z) = -\frac{\varkappa^2}{(2\pi)^2} E_0(z)\int d\rho\delta\varepsilon(\mathbf{r})\exp(i\mathbf{s}\rho),$$

$\mathbf{s} = \varkappa_{\parallel} - \mathbf{k}_{\parallel}$ and the Wronskian has the form $W = -2i\varkappa_z$. $t_1 = -2ik_z t$.

1) Scattering by surface roughness

Assume that $\varepsilon_0(z)$ has the form

$$\varepsilon_0(z) = 1 + \chi_0 \frac{e^{z/a}}{1+e^{z/a}}. \quad (5.7)$$

Then the solutions $u(z)$ and $v(z)$ can be expressed in terms of hypergeometric functions, and in the case of statistically uniform surfaces the expression for the scattering intensity for $z \to -\infty$, according to (5.6) has the form

$$I_1 = I_0\varkappa^4 |t_0|^2 \int d\mathbf{k}_{\parallel} e^{-i(\varkappa_z - \varkappa_z^*)z}\left|\frac{t}{2i\varkappa_z}\right|^2 K(\mathbf{s}), \quad (5.8)$$

where I_0 is the intensity of the incident wave. The coefficient t for a layer of the form (5.7) has the form

$$t = \frac{\Gamma(1-i\varkappa_z a - ik_z a)\,\Gamma(-i\varkappa_z a - ik_z a)}{\Gamma(1-i2k_z a)\,\Gamma(-i2\varkappa_z a)};$$

$$K(\mathbf{s}) = \frac{1}{(2\pi)^2}\int d\rho e^{i\mathbf{s}\rho}\langle\delta\varepsilon(\rho')\,\delta\varepsilon^*(\rho'')\rangle,$$

$$\delta\varepsilon(\rho) = \int_{-\infty}^{\infty} dz\,\delta\varepsilon(\mathbf{r})\,u_0(z)\,u(z),$$

$$u(z) = \left(\frac{e^{z/a}}{1+e^{z/a}}\right)^{i\varkappa_z a}(1+e^{z/a})^{ik_z a} \times F\left(i(\varkappa_z - k_z)a,\ 1+i(\varkappa_z - k_z)a,\ 1-i2k_z a,\ \frac{1}{1+e^{z/a}}\right),$$

where $t_0 = t(\theta_0)$, $u_0(z) = u(z)|_{\theta=\theta_0}$, and $F(\alpha, \beta, \gamma, z)$ is the hypergeometric function. Since in the experiments the reflection intensity is studied as a function of only one of the angular variables (the grazing angle η), we can average over the second angular variable. It is also convenient to go over to a Fourier transformation of the quantity $\delta\varepsilon(z)$.

Expression (5.8) then takes the following form

$$I_1 = I_0\varkappa^4 |t_0|^2 \int_{-\infty}^{\infty} dk_{\parallel} e^{2\varkappa_z'' z}\left|\frac{t}{2i\varkappa_z}\right|^2 K(\mathbf{s}), \quad (5.9)$$

where

$$K(\mathbf{s}) = \int_{-\infty}^{\infty} dk \int_{-\infty}^{\infty} dk' f(k) f^*(k')\cdot\frac{1}{2\pi}\int dx e^{isx}\langle\delta\varepsilon(k)\,\delta^*\varepsilon(k')\rangle,$$

$$f(k) = \int_{-\infty}^{\infty} dz\,u_0(z)\,u(z)\,e^{ikz},$$

$$\delta\varepsilon(k) = \frac{1}{2\pi}\int \delta\varepsilon(z)\,e^{-ikz}\,dz = \frac{t}{2\pi}\frac{|\chi_0|}{k}\frac{e^{-ik\zeta}\,\mathrm{sh}(\pi ka) - \pi ka}{\mathrm{sh}(\pi ka)},$$

and $z = \zeta(x, y)$ is the equation of the surface roughness. If for simplicity we assume that $u_0(z) = e^{i\varkappa_{0z}z}$ and $u(z) = e^{i\varkappa_z z}$, i.e., that these functions have the form of a plane wave, then it is easy to show that $K(s)$ can be approximated by the following expression:

$$K(\mathbf{s}) = \frac{|\chi_0|^2}{(\varkappa_{0z}+\varkappa_z)^2}\left\{\frac{L}{2\sqrt{\pi}}(1-e^{-\sigma^2(\varkappa_{0z}+\varkappa_z)^2})\,e^{-s^2L^2/4} + \left[\frac{e^{-\frac{\sigma^2(\varkappa_{0z}+\varkappa_z)^2}{2}}\,\mathrm{sh}\,\pi a(\varkappa_{0z}+\varkappa_z) - \pi a(\varkappa_{0z}+\varkappa_z)}{\mathrm{sh}\,\pi a(\varkappa_{0z}+\varkappa_z)}\right]^2\delta(s)\right\}, \quad (5.10)$$

where

$$L = \frac{l}{\sqrt{1+\sigma^2(\varkappa_{0z}+\varkappa_z)^2}},$$

l is the characteristic correlation length of the nonuniform surface, and σ is the dispersion. The first term in (5.10) describes the intensity of the nonspecular component in the scattered field, and the second describes the intensity of the specular component.

The degree of surface roughness is defined by the parameter $\theta(\varkappa_{0z} + \varkappa_z)$ which determines the phase difference between the waves reflected from the lower and the upper surfaces of the transition layer. For $\sigma(\varkappa_{0z} + \varkappa_z) \ll 1$, the surface is not very rough, while in the opposite case the surface is very rough. In the first case the width of the angular distribution of the nonspecular reflection, as follows from (5.10), is determined only by the correlation length l, while only the intensity depends on σ. For very rough surfaces both the width of the angular distribution and the intensity depend on the parameter σ/l, which defines the average angle of misorientation of the surface nonuniformities. We shall now estimate the numerical value of σ that corresponds to the condition $\sigma\varkappa_{0z} \sim 1$. Setting $\varkappa_{0z} \sim \varkappa\eta_c$, we obtain for the amplitude of the roughness $d = 2\sigma \approx 200$ Å in the case of Si, i.e., the surface can be considered not very rough if it has a 14th class finish.

Let us now determine the scattering angle dependence of the second factor $|t/2i\varkappa_z|^2$ in the integrand of expression (5.8). The form of this dependence is shown in Fig. 10. This factor is constant in the region $0 \ll \eta \ll \eta_c$ and falls off rapidly on both sides of this interval. Because experimentally the intensity of the reflected field is measured as a function of the grazing angle η, the factor $dk_{\parallel} = d(\varkappa\cos\eta) \approx -\varkappa\eta d\eta$ also plays an extremely important role, i.e., the dependence $I(\eta)$ will be observed to fall off towards small values of η. The overall dependence $I(\eta)$ has the form shown in Fig. 11, where

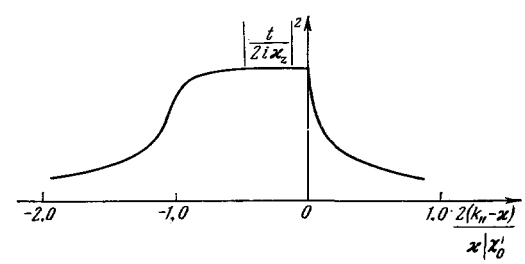

FIG. 10. Interpretation of formula (5.9).

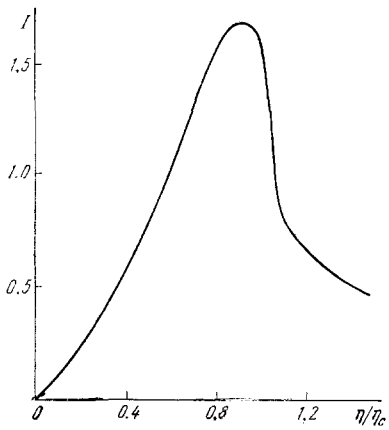

FIG. 11. Form of the angular dependence of the anomalous reflection intensity according to (5.9)–(5.10) for the following values of the parameters: $\sigma = 1000$ Å, $l = 70\,\mu$m, $\eta_0 = 2\eta_c$, and $\eta_c = 15'$.

the following values of the parameters were used: $\sigma = 1000$ Å and $l = 70\,\mu$m. A comparison of Figs. 11 and 8b show that they agree.

We shall now determine the dependence of the intensity of the anomalous reflection on the class of surface roughness. This dependence is completely determined by the first term in expression (5.10). Figure 12a shows the dependence of the integrated intensity of the anomalous reflection on the class of surface roughness.[45] Figure 12b shows for comparison the dependence of the maximum intensity of the anomalous reflection on the class of surface roughness, as calculated from formulas (5.8) and (5.10).

Thus, the above comparison of the experimental data

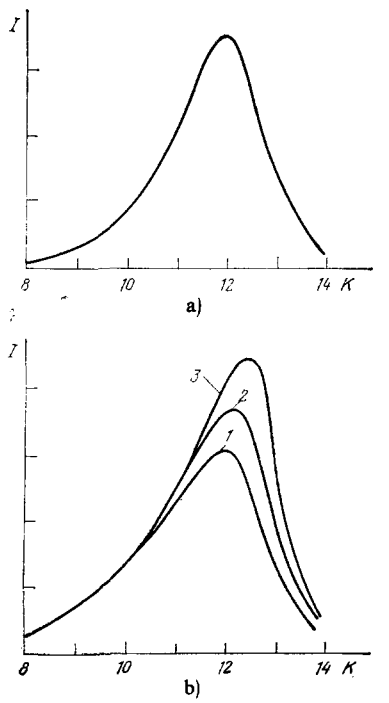

FIG. 12. Dependence of anomalous reflection intensity on class K of surface roughness. a) experiment[45]; b) calculation from formulas (5.9) and (5.10) for the following correlation lengths: 1) 47 μm; 2) 40 μm; 3) 34 μm.

with the results of our theoretical calculations allows us to conclude that the appearance of anomalous reflection in the experiments described in section 4a is due to scattering of the x rays by density fluctuations of the medium within the surface (transition) layer. The formulas presented above make it possible from the angular dependence of the reflection to determine the statistical characteristics of surface nonuniformities.

2) Scattering by bulk nonuniformities in a surface layer

Formula (5.8) will have exactly the same form if the scattering of the x rays occurs also at bulk nonuniformities that are due to radiation damage in the surface layer. The only difference will be in the form of the function $K(\mathbf{s})$, which in this case takes the following form:

$$K(\mathbf{s}) = \frac{1}{(2\pi)^2}\int d\rho e^{i\mathbf{s}\rho}\int_{-\infty}^{\infty} dz\, u_0(z)\, u(z) \times \int_{-\infty}^{\infty} dz'\, u_0^*(z')\, u^*(z')\,\langle \delta\varepsilon(\mathbf{r})\cdot\delta\varepsilon^*(\mathbf{r}')\rangle. \quad (5.11)$$

The correlation function now depends not on two variables, but in general on four:

$$\langle \delta\varepsilon(\mathbf{r})\,\delta\varepsilon^*(\mathbf{r}')\rangle = |\chi_0|^2\langle\xi^2\rangle \exp\left[-\frac{\rho^2}{l^2} - \frac{(z'-z)^2}{a^2} - \frac{(z'+z)^2}{b^2}\right],$$

where $\xi = \delta\varepsilon/|\chi_0|$. It is meaningful to speak of scattering by bulk nonuniformities only when the contribution from scattering by surface nonuniformities is small. According to the estimates of the previous section, this occurs if the surface corresponds to a 14th class finish or better. In this case the transition layer can be replaced by a sharp boundary. Then assuming that $\varkappa a\eta_c \sim \varkappa b\eta_c \gg 1$, we obtain

$$K(s) = \frac{|\chi_0|^2 l}{2\sqrt{\pi}}\langle\xi^2\rangle\frac{1}{|k_{0z}+k_z|^2}e^{-s^2l^2/4}, \quad (5.12)$$

where $k_z = \varkappa\sqrt{\varepsilon - \sin^2\theta}$.

Thus, the functions $K(s)$, which are the Fourier transforms of the correlation functions and determine the form of the angular dependence of the nonspecular reflection, have a similar form both for scattering by surface and bulk nonuniformities.

3) The secondary peak

In formula (5.9) the integration over $k_\parallel$ was carried out from minus to plus infinity. Waves with $|k_\parallel| < \varkappa$ have in the vacuum real projections of the wave vector on the normal to the interface, $\varkappa_z = \sqrt{\varkappa^2 - k_\parallel^2}$, while waves with $k_\parallel > \varkappa$ have imaginary projections. In the latter case the waves in the vacuum will be nonuniform and their amplitudes will fall off exponentially with distance from the interface into the vacuum. The tota intensity of these waves as a function of z is determined by the value of the following integral:

$$I_2(z) = I_0\varkappa^4|t_0|^2\int_{\varkappa}^{\infty} dk_\parallel \left|\frac{t}{2i\varkappa_z}\right|^2 K(s)\, e^{2z\sqrt{k_\parallel^2-\varkappa^2}}.$$

We recall that the vacuum occupies the half-space $z < 0$.

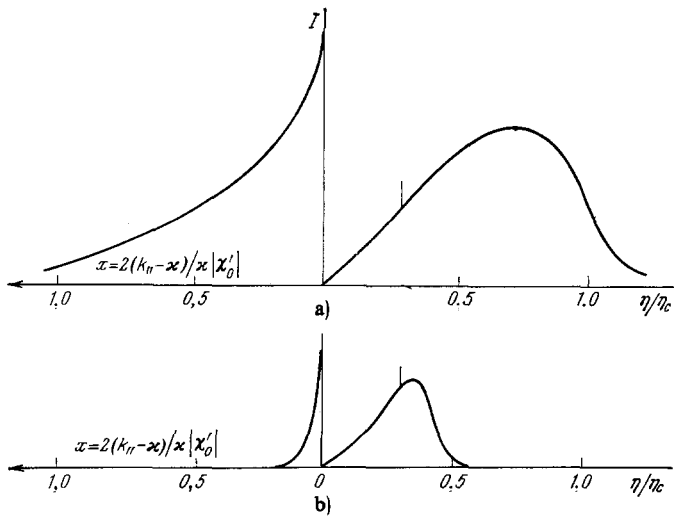

FIG. 13. Form of the nonspecular reflection intensity as a function of scattering angle η (right side of figure) and of $k_\parallel$ for $k_\parallel > \varkappa = \omega/c$ (left side). The calculations were carried out for a silicon crystal for the following parameters: $\eta_0 = 0.3\,\eta_c$, $l = 6.25\,\mu$m (a) and $l = 62.5\,\mu$m (b).

Consequently, if the width of the curve $K(s)$ is much larger than $|k_\parallel - \varkappa_\parallel| \gg \varkappa|\chi_0'|$, then for angles of incidence close to the critical angle, there will be a peak in the intensity of the scattered field at the crystal surface, and its intensity will be determined by that part of the area under the curve in Fig. 10 that lies to the right of the point $k_\parallel = \varkappa$. Figure 13 shows the form of the dependence of the integrand in (5.9) on the exit angle η normalized to η_c in the region $k_\parallel < \varkappa$ (the right half of the figure) and on the variable $x = 2(k_\parallel - \varkappa)/\varkappa|\chi_0'|$ in the region $k_\parallel > \varkappa$ (the left half of the figure. We note that the value $\eta = \eta_c$ corresponds to $x = -1$. In the calculation the function $K(s)$ of the form (5.12) was used, with $l = 6.25\,\mu$m (Fig. 13a) and $l = 62.5\,\mu$m (Fig. 13b).

Thus, our calculations show that the formation of the secondary peak in the experiments described in section 4b, paragraph 5 can be explained by small-angle scattering in the surface layer. This is due to scattering both by bulk nonuniformities and by surface roughness, where the dominant contribution is evidently from the former mechanism. The dependence of the angular distribution on the distance of the irradiated region from the edge of the crystal can be explained by a displacement of the scattered beam that impinges from the medium onto the interface with the vacuum and undergoes reflection. If we use formula (2.7), then for $\eta_{cA} = \sqrt{|\chi_A'|}$, where χ_A is the polarizability of air, we obtain

$$l = \frac{2\lambda}{\pi\sqrt{|\chi_0'|\,|\chi_A''|/2}}.$$

For characteristic values of the parameters we obtain $l \approx 0.5$ cm, which agrees with the experimental data.

6. STUDIES OF THE EXTENDED FINE STRUCTURE IN THE REFLECTION SPECTRA

Studies of the extended fine structure in reflection spectra significantly widen the possibilities for the application of EXAFS spectroscopy (see the review of Ref. 47) to the investigation of the structure of surface layers, thin films, and interfaces. The basis of EXAFS spectroscopy is the study of the fine structure of the absorption energy spectra from the absorption edge upwards towards higher energy. This structure is due to the dependence of the final state wave function of the photoelectron on the photoelectron energy and is related to the scattering of the photoelectron by the nearest neighbor atoms. The phase of this scattering depends on the type of neighboring atoms and their arrangement relative to the atom whose absorption edge is being studied. Therefore, EXAFS data allows inferences to be drawn concerning the structure of the short range order.

In transmission experiments the crystal thickness that is optimal for producing the necessary contrast is close to the reciprocal of the absorption coefficient. This has placed a limitation on the use of the method for the study of thin films. Methods that are associated with detecting secondary processes have substantially reduced sensitivities. Therefore the observation of oscillations in spectra of specular reflection at grazing angles of incidence[48] has opened up wide possibilities in the study of thin films. While the first experiments used synchrotron radiation, later it was shown to be possible to use ordinary x-ray tubes.[49–53]

The possibility of varying the penetration depth of the wave in the medium by varying the angle of incidence permits the study of the variation of the short range order structure with distance from the interface. The penetration depth, as the grazing angle goes from zero to η_c, varies, as we have noted above, from several tens to several thousands of angstroms. Ion-implanted silicon crystals have been studied by this method in Ref. 53, and it was shown that there is a substantial change in the short range order structure between a penetration depth of the order 40 Å, (angle of incidence 7′) and 1000 Å (angle of incidence 9′).

If the surface layer of the material studied is nonuniform, then information on the short range order structure in films of different thicknesses can be obtained by studying the energy spectra at various parts of the angular distribution. Actually, to each value of the exit angle η corresponds a particular projection $k_\parallel$ of the wave vector on the interface: $\eta = \sqrt{\varkappa^2 - k^2}/\varkappa$. On the other hand, to each value of $k_\parallel$ in

the range $0 < \eta < \eta_c$ there corresponds a particular attenuation increment $\Gamma = \sqrt{k_\parallel^2 - \varkappa^2\langle\varepsilon\rangle}$ in the material, and, consequently, a particular escape depth $l = 1/\Gamma$. In Ref. 54 the appearance of a secondary peak in the angular dependence was utilized, and the energy structure within the broadened specular peak and the secondary peak was studied. Germanium crystals with oxide films were used as samples. Nonuniformity of the oxide films evidently was the reason for the appearance of the secondary peak. The Fourier spectrum of the fine structure of the specular reflection corresponded to the germanium structure. In the scattered field correlation with the structure of the germanium environment in GeO_2 is observed and there is a peak that corresponds to the Ge-Ge spacing.

CONCLUSIONS

In summary, we can conclude that the use of grazing angles of incidence of x rays (and also gamma rays, neutrons, ions) opens up new prospects in the investigation of thin films. X-ray diffraction at grazing angles of incidence has become a universal tool for the study of two-dimensional structures whose thickness is a few atomic layers. In this area the method that is the most developed is that of noncoplanar two-wave diffraction, which has been used for the study of such delicate effects as the reconstruction of metal and semiconductor surfaces and two-dimensional phase transitions. The possibility of studying single layers of biological macromolecules deposited on a solid substrate is being considered.[55] Noncoplanar diffraction is opening up greater possibilities in the study of interfaces within multilayer structures, including those beneath amorphous films.

The first experiments have been carried out in the investigation of dynamic effects in noncoplanar two-wave diffraction geometry. Further developments of this method will no doubt provide new information on the structure of crystal surfaces, information that cannot be obtained by other surface diagnostic methods.[55] One of the clear manifestations of dynamic diffraction at a surface is the possibility of exciting diffracted x-ray surface waves.

The investigation of total external reflection in the absence of diffraction has also received a new surge of development. For instance, investigations of the energy spectra of extended fine structure in reflection have shown the possibility of studying the short range order structure in near-surface regions consisting of a few atomic layers. The simplicity in varying the thickness of the investigated layer from a few to hundreds or thousands of monolayers by varying the angle of incidence is of considerable significance. The study of the structure of damaged surface layers must be associated with the angle-dependent structure of reflected waves. In the article above we have attempted to show that the statistical characteristics of nonuniformities can be determined on the basis of a simple analysis.

Methods based on a combination of those described above are believed to hold considerable promise. Such combinations may provide information on short and long range order both for ideal and for mildly damaged crystals.

Thus, there is every reason to expect in the near future vigorous progress in the development of x-ray optical methods in surface diagnostics.

The author wishes to express his deep gratitude to S. A. Akhmanov, É. K. Kov'ev, Yu. V. Ponomarev, and Yu. A. Turutin for many discussions of the problems treated in this review.

[1]Z. G. Pinsker, Rentgenovskaya kristallooptika [X-ray Crystal-Optics] Nauka, M., 1982.
[2]P. Farwig and H. W. Schurman, Z. Phys. **204**, 489 (1967).
[3]S. Kishino, J. Phys. Soc. Jpn. **31**, 1168 (1971).
[4]S. Kishino and K. Kohra, Jpn. J. Appl. Phys. **10**, 551 (1971)
[5]S. Kishino, A. Noda, and K. Kohra, J. Phys. Soc. Jpn. **33**, 158 (1972).
[6]T. Bedynska, Phys. Status Solidi A **19**, 365 (1973); Phys. Status Solidi A **25**, 405 (1974).
[7]F. Rustichelli, Phil Mag. **31**, 1 (1975).
[8]S. Mazkedian and F. Rustichelli, Solid State. Commun. **17**, 609 (1975).
[9]O. Brümmer, Phys. Status Solidi A **33**, 587 (1976).
[10]O. Brümmer, H. -R. Höche, and J. Nieber, Phys. Status Solidi A **37**, 529 (1976).
[11]O. Brümmer, H. -R. Höche, and J. Nieber, Phys. Status Solidi A **46**, K131 (1978).
[12]J. Härtwig, Phys. Status Solidi A **37**, 417 (1976).
[13]J. Härtwig, Phys. Status Solidi A **42**, 495 (1977).
[14]J. Härtwig, Exp. Tech. Phys. **26**, 131 (1978).
[15]T. Takahashi and S. Kikuta, J. Phys. Soc. Jpn. **46**, 1608 (1979).
[16]G. Balestrino, S. Lagomarsino, L. Mastrogiacomo, F. Scarinci, and A. Tucciarone, Thin Solid Films **78**, 327 (1981).
[17]A. Fukuhara and Y. Takano, J. Appl. Cryst. **10**, 287 (1977).
[18]S. W. Wilkins, Acta Crystallogr. Sect. A **36**, 143 (1980).
[19]O. Brümmer, H. -R. Höche, and J. Nieber, Z. Naturforsch. Teil A **37**, 517 (1982).
[20]V. M. Kaganer, V. L. Indenbom, M. Vrana, and B. Chalupa, Phys. Status. Solidi A **71**, 371 (1982).
[21]F. Eichhorn, J. Kulda, and P. Mikula, Phys. Status Solidi A **80**, 483 (1983).
[22]A. Zeilinger and T. J. Beatty, Phys. Rev. B **27**, 7239 (1983).
[23]A. V. Andreev and E. K. Kov'ev, Izv. Akad. Nauk SSSR Ser Phys. **47**, 1984 (1983) [Bull. Acad. Sci. USSR Phys. Ser. No. 10, p. 101 (1984)].
[24]B. G. Baryshevskiĭ, Pis'ma Zh. Tekh. Fiz. **2**, 112 (1976) [Sov. Tech. Phys. Lett. **2**, 43 (1976)].
[25]W. C. Marra, P. Eisenberger, and A. Y. Cho, J. Appl. Phys. **50**, 6927 (1979).
[26]P. Eisenberger and W. C. Marra, Phys. Rev. Lett. **46**, 1081 (1981).
[27]W. C. Marra, P. H. Fuoss, and P. Eisenberger, Phys. Rev. Lett. **49**, 1169 (1982).
[28]I. K. Robinson, Phys. Rev. Lett. **50**, 1145 (1983).
[29]A. V. Andreev, E. K. Kov'ev, Yu. A. Matveev, and Yu. V. Ponomarev, Pis'ma Zh. Eksp. Teor. Fiz. **35**, 412 (1982) [JETP Lett. **35**, 508 (1982)].
[30]G. H. Vineyard, Phys. Rev. B **26**, 4146 (1982).
[31]A. M. Afanas'ev and M. K. Melkonyan, Acta Crystallogr. Sect. A **39**, 207 (1983).
[32]P. A. Aleksandrov, A. M. Afanas'ev, and M. K. Melkonyan, Fiz. Tverd. Tela (Leningrad) **25**, 1003 (1983) [Sov. Phys. Solid State **25**, 578 (1983)].
[33]A. L. Golovin and R. M. Imamov, Phys. Status Solidi A **77**, K91 (1983).
[34]M. A. Andreeva and R. N. Kuz'min, Solid State Commun. **49**, 743 (1984).
[35]V. M. Sinaĭskiĭ and V. I. Sidenko, Prib. Tekh. Éksp. No. 6, p. 5 (1974) Instrum. Exp. Tech. (USSR).
[36]Y. Yoneda, Phys. Rev. **131**, 2010 (1963).
[37]E. K. Kov'ev and Yu. A. Matveev, Fiz. Tverd. Tela (Leningrad) **23**, 587 (1981) [Sov. Phys. Solid State **23**, 331 (1981)].
[38]A. N. Nigam, Phys. Rev. **138A**, 1189 (1965).
[39]B. E. Warren and J. S. Clarke, J. Appl. Phys. **36**, 324 (1965).
[40]O. J. Guentert, J. Appl. Phys. **36**, 1361 (1965).
[41]J. B. Bindell and N. Wainfan, J. Appl. Cryst. **3**, 503 (1970).
[42]B. M. Rovinskiĭ, V. M. Sinaĭskiĭ, and V. I. Sidenko, Fiz. Tverd. Tela (Leningrad) **14**, 409 (1972) [Sov. Phys. Solid State **14**, 340 (1972)].
[43]A. G. Tur'yanovskiĭ and K. V. Kiseleva, Kr. soobshch. fiz. (FIAN SSSR) [Short Communications in Physics (P. N. Lebedev Institute of Physics of the Academy of Sciences of the USSR)] No. 8, p. 20 (1977).
[44]K. V. Kiseleva and A. G. Tur'yanovskiĭ, Kr. soobshch. fiz. (FIAN SSSR) [Short Communications in Physics (P. N. Lebedev Institute of Physics of the Academy of Sciences of the USSR)] No. 8, p. 25 (1977).

[45]K. V. Kiseleva and A. G. Tur'yanovskiĭ, Preprint FIAN SSSR No. 34, Moscow (1979) [Preprint of the P. N. Lebedev Institute of Physics of the Academy of Sciences of the USSR].
[46]P. V. Petrashen', E. K. Kov'ev, F. I. Chukhovskiĭ, and Yu. L. Degtyarev, Fiz. Tverd. Tela (Leningrad) **25**, 1211 (1983) [Sov. Phys. Solid State **25**, 695 (1983)].
[47]P. A. Lee, P. H. Citrin, P. Eisenberger, and B. M. Kincaid, Rev. Mod. Phys. **53**, 769 (1981).
[48]R. Barchewitz, M. Cremonese-Visicato, and G. Onori, J. Phys. C **11**, 4439 (1978).
[49]G. Martens and P. Rabe, Phys. Status Solidi A **57**, K31 (1980).
[50]G. Martens and P. Rabe, Phys. Status Solidi A **58**, 415 (1980).
[51]G. Martens and P. Rabe J. Phys. C **14**, 1523 (1981).
[52]G. Martens and P. Rabe, J. Phys. C **13**, L913 (1980).
[53]Yu. V. Ponomarev and Yu. A. Turutin, Zh. Tekh. Fiz. **53**, 2398 (1983) [Sov. Phys. Tech. Phys. **28**, 1474 (1983)].
[54]Yu. V. Ponomarev and Yu. A. Turutin, Zh. Tekh. Fiz. **53**, 1652 (1983) [Sov. Phys. Tech. Phys. **28**, 1018 (1983)].
[55]A. L. Robinson, Science **221**, 1274 (1983).
[56]A. V. Andreev, S. A. Akhmanov, and É. K. Kov'ev, Izv. Akad. Nauk SSSR Ser. Fiz. **47**, 1898 (1983) [Bull. Acad. Sci. USSR Phys. Ser. No. 10, p. 21 (1983)].
[57]A. V. Andreev and S. A. Akhmanov, Preprint fiz. f-ta MGU No. 6, Moscow (1981) Preprint of the Physics Faculty, Moscow State University.
[58]G. S. Baldwin, J. C. Solem, and V. I. Goldanskii, Rev. Mod. Phys. **53**, pt. I 687 (1981).
[59]B. W. Batterman, Phys. Rev. **133A**, 759 (1964).
[60]J. A. Golovchenko, B. W. Batterman, and W. L. Brown, Phys. Rev. B **10**, 4239 (1974).
[61]M. V. Kruglov, E. A. Sozontov, V. N. Shchemelev, and B. G. Zakharov, Kristallografiya **22**, 693 (1977) [Sov. Phys. Crystallogr. **22**, 397 (1977)].
[62]J. A. Golovchenko, J. R. Patel, D. R. Kaplan, P. L. Cowan, and M. Bedzyk, Phys. Rev. Lett. **49**, 560 (1982).
[63]V. G. Kohn, M. V. Kovalchuk, R. M. Imamov, V. G. Zakharov, and E. F. Lobanovich, Phys. Status Solidi A **71**, 603 (1982).
[64]R. S. Becker, J. A. Golovchenko, and J. R. Patel, Phys. Rev. Lett. **50**, 153 (1983).
[65]I. K. Solomin and M. V. Kruglov, Fiz. Tverd. Tela (Leningrad) **26**, 519 (1984) [Sov. Phys. Solid State **26**, 310 (1984)].
[66]G. Martens, P. Rabe, G. Tolkiehn, and A. Werner, Phys. Status Solidi A **55**, 105 (1979).
[67]J. Stöhr, L. Johanson, I. Lindau, and P. Pianetta, Phys. Rev. B **20** 664 (1979).
[68]P. H. Citrin, P. Eisenberger, and R. C. Hewitt, Phys. Rev. Lett. **41**, 309 (1978).
[69]J. A. Del Cueto and N. J. Shevchik, J. Phys. C **11**, L833 (1978).

Translated by J. R. Anderson